The Metal Ion Binding Properties of Calreticulin Modulate Its Conformational Flexibility and Thermal Stability†

Zhenjie Li,‡ Walter F. Stafford,§ and Marlène Bouvier*,‡

School of Pharmacy, University of Connecticut, Storrs, Connecticut 06269, and Boston Biomedical Research Institute, Watertown, Massachusetts 02472

Received May 9, 2001; Revised Manuscript Received June 25, 2001

ABSTRACT: Calreticulin (CRT) is a soluble chaperone involved in the conformational maturation of glycoproteins in the endoplasmic reticulum. Using biochemical and biophysical techniques including circular dichroism, proteolysis, and analytical ultracentrifugation, we have determined the effects of calcium and zinc ions on the structural properties of human CRT. Circular dichroism analysis has shown that the binding of calcium and zinc ions to CRT induces no significant changes in the secondary structure of the protein but affects in very distinct ways the local tertiary packing of these elements. More specifically, these studies have revealed that CRT adopts a more rigid and thermally stable structure upon binding calcium ions and a more loosely packed and thermally destabilized structure upon binding zinc ions. Consistent with these results, proteolysis experiments demonstrated that the intrinsic conformational flexibility of CRT can be modulated toward either a decrease or an increase in susceptibility to cleavage by chymotrypsin upon binding calcium or zinc ions, respectively. Results from sedimentation analysis indicated that the global three-dimensional structure of CRT is essentially unchanged upon binding calcium ions. In marked contrast, CRT self-associates reversibly to form dimers upon binding zinc ions. Collectively, our results provide evidence that calcium and zinc ions induce strikingly different changes in the biochemical and structural properties of CRT.

Calreticulin (CRT)[1] is a 46.8 kDa chaperone involved in the conformational maturation of glycoproteins in the lumen of the endoplasmic reticulum (ER). Along with specialized enzymes, CRT forms a unique system that ensures the structural integrity of glycoproteins prior to their export out of the ER. Although it is clearly established that the chaperone action of CRT is exerted through association with specific immature *N*-linked glycans on nascent proteins (*1*−*4*), it is now recognized that CRT may also act as a more classical chaperone as evidenced by its ability to suppress the aggregation of unfolded proteins in in vitro assays (*5, 6*).

Based on sequence prediction plots, the primary structure of CRT has been divided into three distinct domains with somewhat loosely defined boundaries (*7, 8*): the N-domain (residues 1−180), the P-domain (residues 181−290), and the C-domain (residues 291−400). In brief, the N-domain is highly conserved among CRT species (*9*) and contains a low-affinity, high-capacity zinc binding site (K_d = 310 μM and 14 mol of zinc/mol of CRT) (*10*). It has been shown that the N-domain mediates interactions between CRT and the ER folding catalysts PDI and ERp57 (*11, 12*). The central P-domain contains two proline-rich repeat sequences, type 1 and type 2 motifs, that have been shown from recent NMR studies (*13, 14*) to be primarily structural motifs allowing the P-domain to adopt a unique hairpin-type fold in solution. Evidence has been provided that the P-domain is likely to contain a high-affinity calcium binding site (K_d = 0.05−10 μM and 1 mol of calcium/mol of CRT) (*10, 15*−*19*) and has been implicated in the binding of isolated oligosaccharides as well as glycoprotein ligands in in vitro assays (*20, 21*). Finally, the P-domain has also been implicated in complex formation between CRT and PDI (*12*). The C-domain is characterized by a high content of acidic residues (*7, 8, 17, 22*) which is consistent with the location of a low-affinity, high-capacity calcium binding site (K_d = ∼1−2 mM and ∼25−50 mol of calcium/mol of CRT) (*16, 17, 23*). The C-domain contains the ER-retrieval sequence and has been shown to regulate, in some way, calcium-dependent interactions between CRT and PDI or ERp57 (*11, 12*). Although the spatial organization of the N-, P-, and C-domains of CRT has not yet been described, it has been shown from sedimentation analysis that the protein adopts an elongated shape in solution (*24, 25*), a characteristic that can be attributed, at least in part, to the extended hairpin structure of the P-domain (*13, 14*). The elongated molecular shape of

† This work was supported by NIH Grant AI45070 (M.B.), NSF Grant BIR-9513060 (W.F.S.), and the Graduate School of the University of Connecticut (Z.L.).

* To whom correspondence should be addressed at the University of Connecticut, School of Pharmacy, 372 Fairfield Rd. U-92, Storrs, CT 06269. Phone: (860) 486-4355; Fax: (860) 486-4998; E-mail: bouvier@uconnvm.uconn.edu.

‡ University of Connecticut.

§ Boston Biomedical Research Institute.

[1] Abbreviations: CD, circular dichroism; CRT, calreticulin; EDTA, ethylenediaminetetraacetic acid; EGTA, ethylene glycol bis(2-aminoethyl ether)-*N*,*N*,*N*′,*N*′-tetraacetic acid; ER, endoplasmic reticulum; GST, glutathione *S*-transferase; MALDI, matrix-assisted laser desorption ionization; MW, molecular mass; NMR, nuclear magnetic resonance; PAGE, polyacrylamide gel electrophoresis; PDI, protein disulfide isomerase; SDS, sodium dodecyl sulfate; T_m, thermal denaturation midpoint temperature; UV, ultraviolet.

10.1021/bi010948l CCC: $20.00
Published on Web 08/23/2001

CRT strongly suggests that the protein is characterized by high intrinsic structural plasticity which might be required for its chaperone function (*13*, *24*).

In this paper, we report on the roles that calcium and zinc ions play in modulating the intrinsic structural plasticity of CRT. Using a series of biochemical and biophysical approaches, we describe how these divalent metal ions alter the structural properties of CRT in a manner that is consistent with the formation of two very distinct binding sites possibly directed at the expression of a high-affinity calcium-dependent lectin function or a more classical, low-affinity zinc-dependent chaperone function. The notion that the structural properties of CRT are highly dependent upon interactions with calcium and zinc ions suggests the possible importance of these metal ions in modulating the function of CRT in the cellular environment of the ER.

EXPERIMENTAL PROCEDURES

Expression and Purification of CRT. Human CRT was expressed in the *E. coli* strain BNN103 based on a glutathione *S*-transferase (GST) fusion protein system as previously described (*24*). In brief, the crude GST−CRT fusion protein was purified at 4 °C on a glutathione−Sepharose 4B affinity column, dialyzed, and digested with Factor Xa, leaving four additional amino acid residues (G-I-P-G) at the N-terminus of CRT. The proteolytic mixture was then directly applied onto the glutathione−Sepharose 4B affinity column, and the flow-through containing CRT was purified on an Uno Q-6 (Bio-Rad) FPLC ion-exchange column. Each new batch of purified CRT was characterized by N-terminal amino acid sequencing and by MALDI mass spectrometry to confirm the specificity of the Factor Xa cleavage site and the molecular mass (MW) of the protein, respectively. Concentrations of the stock CRT solutions, in 20 mM Hepes pH 7.5, 150 mM NaCl, were determined at 280 nm by the Edelhoch's method (*26*) using a calculated extinction coefficient of 80 630 M^{-1} cm^{-1} based on the tryptophan, tyrosine, and cystine content.

Circular Dichroism Measurements. CD experiments were carried out using a Jasco-715 spectropolarimeter equipped with a thermoelectric temperature controller. CRT solutions in 20 mM Hepes, pH 7.0, 200 mM NaCl containing 2 mM EDTA or 50−1000 μM $CaCl_2/ZnCl_2$ and in 20 mM Hepes, pH 7.0, 200 mM NaCl, 3 mM $MgCl_2$ containing one of the following additives, 1 mM EGTA, 50−2000 μM $CaCl_2$, or 50−400 μM $ZnCl_2$, were used for all measurements. The near- and far-ultraviolet (UV) CD spectra were recorded at 25 °C in the range 320−250 and 250−203 nm, respectively, as described previously (*24*). Protein concentrations were 0.4 and 0.2 mg/mL for the near- and far-UV measurements, respectively. Thermal denaturation curves were obtained by monitoring the change in ellipticity at 280 nm in the range 4−65 °C using a scan rate of 40 °C/h and a 1 cm path length cuvette with a protein concentration of 0.4 mg/mL. The thermal denaturation midpoint temperatures (T_m) were determined by fitting the denaturation curves to an equation describing a two-state denaturation process as described previously (*27*, *28*). Ellipticities are expressed on a molar residue basis or as fraction of folded protein.

Proteolysis. Digests of CRT (0.44 mg/mL) by chymotrypsin (Life Technologies) were carried out at 25 °C using an enzyme:substrate ratio of 1:150 (w/w) in 20 mM Hepes, pH 7.0, 200 mM NaCl, 2 mM EDTA and in 20 mM Hepes, pH 7.0, 200 mM NaCl, 3 mM $MgCl_2$ containing one of the following additives: 1 mM EGTA, 50−1000 μM $CaCl_2$, 400 μM $ZnCl_2$, or 50 μM $CaCl_2$/400 μM $ZnCl_2$. Aliquots were taken at different times from the reaction mixtures, and proteolysis was terminated by the addition of SDS loading buffer and boiling samples to 100 °C. Samples were analyzed by SDS−PAGE (12%) and electroblotted onto a poly(vinylidene difluoride) membrane (Millipore) for N-terminal amino acid sequencing analyses. Amino acid residues are numbered according to the sequence of full-length recombinant CRT(1−400) without including the additional four N-terminal residues (see above).

Analytical Ultracentrifugation. Sedimentation equilibrium and velocity experiments were carried out at 25 °C as described previously (*24*). A stock solution of CRT at approximately 2 mg/mL was dialyzed for at least 24 h in 20 mM Hepes, pH 7.0, 200 mM NaCl, 2 mM EDTA and in 20 mM Hepes, pH 7.0, 200 mM NaCl, 3 mM $MgCl_2$ containing one of the following additives: 1 mM EGTA, 50−1000 μM $CaCl_2$, 400 μM $ZnCl_2$, or 50 μM $CaCl_2$/400 μM $ZnCl_2$, prior to analysis. In addition, a series of dilutions of CRT in the range 0.1−1.0 mg/mL were prepared using the dialysate as diluent for buffer conditions 20 mM Hepes, pH 7.0, 200 mM NaCl, 3 mM $MgCl_2$ containing 400 μM $ZnCl_2$ or 50 μM $CaCl_2$/400 μM $ZnCl_2$. For sedimentation equilibrium runs, six-channel external loading centerpieces (Beckman Coulter part numbers 366755 and 368115) were used. Sedimentation velocity patterns were analyzed using time-derivative analysis (*29*). For sedimentation equilibrium runs, an optical blank run of water versus water was performed to correct for optical inhomogeneities in the cell windows and lenses. Blanks were performed both before and after the run at the expected and actual speeds, respectively. The blank after the run was performed by rinsing the cell with buffer and water to remove all protein. The two blanks were compared to check for any change in the cell components. The blank was subtracted point by point from the run. Sedimentation equilibrium data were analyzed by global fitting combined data from three loading concentrations and two speeds as described previously (*30*). The values of the partial specific volume and hydration are given in Table 2.

RESULTS

Circular Dichroism Measurements. CD spectroscopy was used to determine the calcium- and zinc-dependent structural properties of CRT by recording near- and far-UV spectra at 25 °C between 320 and 250 nm and 250 and 203 nm, respectively (Figure 1A,C). Thermal denaturation curves were recorded at 280 nm in the temperature range 4−65 °C (Figure 1B). CD measurements were done in 20 mM Hepes, pH 7.0, 200 mM NaCl, 2 mM EDTA and in 20 mM Hepes, pH 7.0, 200 mM NaCl, 3 mM $MgCl_2$ containing one of the following additives: 1 mM EGTA, 50−2000 μM $CaCl_2$, or 50−400 μM $ZnCl_2$. The addition of high concentrations of magnesium ions in buffers for CD experiments allowed discrimination between the high- and low-affinity calcium binding sites of CRT. It is known that magnesium ions do not compete for the high-affinity calcium binding site (*10*, *18*, *25*, and this study), but a weak competing effect has been

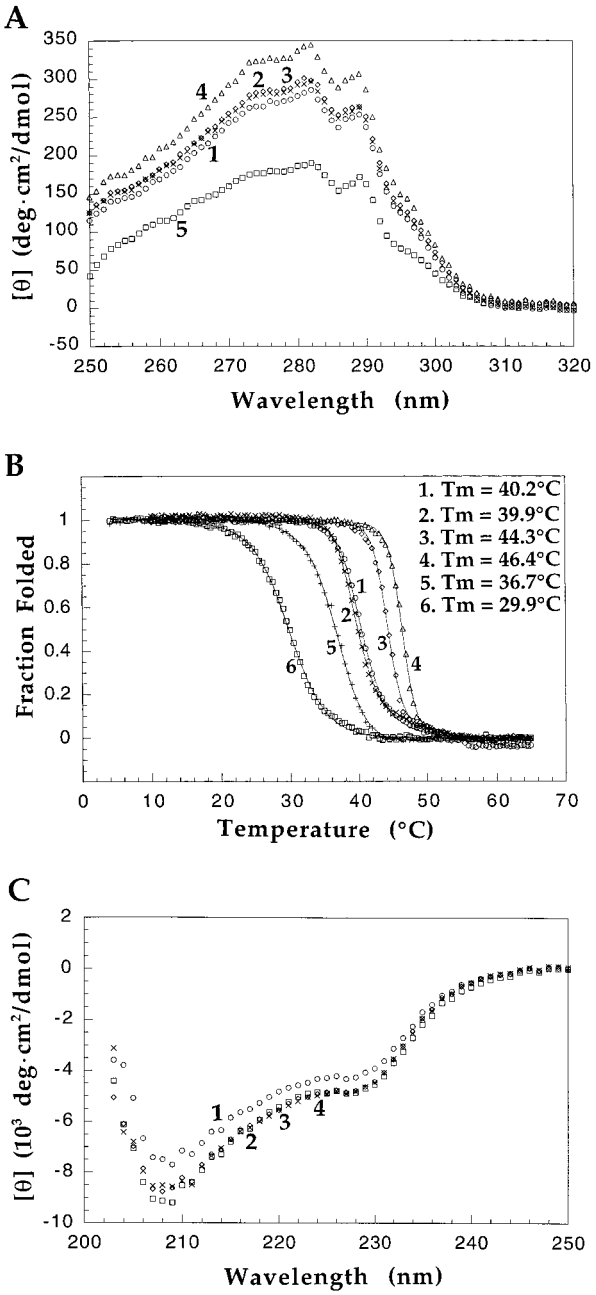

FIGURE 1: (A) Near-UV CD spectra (320−250 nm) of CRT at 25 °C. Protein concentrations were 0.4 mg/mL in 20 mM Hepes, pH 7.0, 200 mM NaCl, 2 mM EDTA (spectrum 1) and in 20 mM Hepes, pH 7.0, 200 mM NaCl, 3 mM $MgCl_2$ containing one of the following additives: 1 mM EGTA (spectrum 2), 50 μM $CaCl_2$ (spectrum 3), 1000 μM $CaCl_2$ (spectrum 4), or 400 μM $ZnCl_2$ (spectrum 5). A 1 cm path length cuvette was used to record the spectra. (B) Thermal denaturation curves (4−65 °C) of CRT obtained by monitoring the change in CD signal at 280 nm. Protein concentrations were 0.4 mg/mL in 20 mM Hepes, pH 7.0, 200 mM NaCl, 2 mM EDTA (curve 1) and in 20 mM Hepes, pH 7.0, 200 mM NaCl, 3 mM $MgCl_2$ containing one of the following additives: 1 mM EGTA (curve 2), 50 μM $CaCl_2$ (curve 3), 1000 μM $CaCl_2$ (curve 4), 50 μM $ZnCl_2$ (curve 5), or 400 μM $ZnCl_2$ (curve 6). A 1 cm path length cuvette was used to record the denaturation curves. The theoretical lines through the data points were generated by fitting the denaturation curves to an equation describing a two-state denaturation process (*27, 28*). (C) Far-UV CD spectra (250−203 nm) of CRT at 25 °C. Protein concentrations were 0.2 mg/mL in 20 mM Hepes, pH 7.0, 200 mM NaCl, 2 mM EDTA (spectrum 1) and in 20 mM Hepes, pH 7.0, 200 mM NaCl, 3 mM $MgCl_2$ containing one of the following additives: 1 mM EGTA (spectrum 2), 50 μM $CaCl_2$ (spectrum 3), or 400 μM $ZnCl_2$ (spectrum 4). A 1 mm path length cuvette was used to record the spectra.

reported for the low-affinity calcium binding site (reported as "data not shown") (*17*).

Figure 1A shows that apo CRT (spectrum 1) is characterized by strong spectral features in the near-UV region, suggesting that the large number of aromatic residues in CRT (11% of the total amino acid sequence) reside in an overall well-ordered asymmetric environment. These features are essentially unchanged by the addition of 3 mM $MgCl_2$ (spectrum 2) except for a small, but noticeable, increase in molar ellipticity. Occupancy of the high-affinity calcium site (spectrum 3) causes no apparent increase in molar ellipticity in comparison to the magnesium-saturated form of CRT (spectrum 2). Interestingly, binding of calcium ions at the low-affinity site (spectrum 4) causes a noticeable increase in molar ellipticity, suggesting a change in the asymmetric environment of particular aromatic residues possibly due to the formation of specific tertiary interactions in the protein. In marked contrast, the addition of 400 μM $ZnCl_2$ (spectrum 5) significantly reduces the intensity of the near-UV CD spectrum, in comparison to the magnesium-saturated form of CRT (spectrum 2), while the overall spectral features are mostly unchanged. These results suggest that the binding of zinc ions to CRT causes structural rearrangements that considerably weaken the tertiary packing of the protein. These results are consistent with fluorescence studies showing that the binding of zinc ions to CRT triggers significant movement of tryptophan residues into the solvent (*5, 10, 18*). Although these authors (*10, 18*) also reported a minor movement of tryptophan residues away from the solvent upon calcium binding at the high-affinity site, these structural effects are mostly undetected in the near-UV CD spectrum (spectrum 3, but also see below).

To further probe the structural effects of calcium and zinc binding to CRT, thermal denaturation curves were recorded at 280 nm (Figure 1B) as previously described (*24*). Results show that the thermal denaturation curve of apo CRT (curve 1) is characterized by a single, sharp transition centered at a relatively low T_m = 40.2 °C. These characteristics are unchanged by the addition of 3 mM $MgCl_2$ (curve 2). Interestingly, occupancy of the high-affinity calcium site by the addition of 50 μM $CaCl_2$ (curve 3) increases the thermal stability of CRT to T_m = 44.3 °C, in comparison to the magnesium-saturated form of CRT (curve 2), as well as sharpens to some extent the denaturation transition. This effect is calcium concentration-dependent since binding of calcium ions at the low-affinity site (curve 4) further increases the thermal stability of CRT to T_m = 46.4 °C. No increase in thermal stability could be detected by the addition of 2000 μM $CaCl_2$ (data not shown). In marked contrast, the addition of 50 μM $ZnCl_2$ (curve 5) decreases the thermal stability of CRT to T_m = 36.7 °C, in comparison to the magnesium-saturated form of CRT (curve 2), and broadens the denaturation transition. Consistent with this trend, an increase to 400 μM $ZnCl_2$ (curve 6) further destabilizes the protein to a low T_m = 29.9 °C as well as significantly broadens the denaturation transition. Collectively, these thermal denaturation curves provide evidence that calcium and zinc ions modulate in vitro the thermal stability of CRT in markedly opposite ways, with calcium being a stabilizing ion and zinc being a destabilizing ion. Furthermore, since the steepness of thermal denaturation transitions is related to the magnitude of the change in enthalpy upon unfolding,

results indicate that binding of calcium ions to CRT (curves 3 and 4) causes the protein to unfold with a higher enthalpy of denaturation than that for binding of zinc ions (curves 5 and 6). The underlying structural significance of these differences is consistent with CRT having a more rigid and well-packed tertiary structure upon binding calcium ions and a more relaxed tertiary structure upon binding zinc ions.

Interestingly, while occupancy of the high-affinity calcium site in CRT changes the midpoint temperature and steepness of the thermal denaturation transition (curve 3 in Figure 1B), the near-UV CD spectrum remains essentially unchanged (spectrum 3 in Figure 1A). These observations strongly suggest that the calcium-induced ordering of CRT occurs at a site that is highly colocalized with the high-affinity calcium binding site such that minor, but apparently critical, structural rearrangements take place. On the other hand, while occupancy of the low-affinity calcium site in CRT further increases the thermal stability of the protein (curve 4 in Figure 1B), this effect is, in this particular case, accompanied by a noticeable increase in molar ellipticity in the near-UV region (spectrum 4 in Figure 1A). These results suggest that a somewhat more delocalized region of CRT is involved in these structural rearrangements. Similarly, since changes in the thermal denaturation curve of CRT upon adding 400 μM $ZnCl_2$ (curve 6 in Figure 1B) were accompanied by a significant decrease in the intensity of the near-UV region (spectrum 5 in Figure 1A), these results also suggest that a more delocalized region of CRT is implicated in this zinc-induced partial disordering.

Finally, to determine whether the addition of 3 mM $MgCl_2$, 50 μM $CaCl_2$, or 400 μM $ZnCl_2$ to CRT changes secondary structure elements, CD spectra in the far-UV region were recorded at 25 °C (Figure 1C). Results show that in comparison to apo CRT (spectrum 1), the magnesium-saturated form of CRT (spectrum 2) shows only a minor increase in molar ellipticity while retaining identical spectral features. No apparent spectral difference could be observed upon occupancy of the high-affinity calcium site (spectrum 3) or the low-affinity zinc binding site (spectrum 4) in comparison to the magnesium-saturated form of CRT (spectrum 2). These results suggest that elements of secondary structures in apo CRT are mostly unchanged upon interactions with these ions, which is consistent with published data (*11*, *19*, *31*). It is important to mention that the buffers used in these experiments preclude recording data below 203 nm, thus reducing the amount of information available for more accurate computer-based secondary structure predictions.

Taken together, CD analysis has shown that the binding of calcium and zinc ions to CRT induces no significant changes in the secondary structure of the protein but affects in very distinct ways the local tertiary packing of these elements and the thermal stability of the protein.

Proteolysis of CRT by Chymotrypsin. To further understand the effect of calcium and zinc ions on the structural properties of CRT, the proteolytic susceptibility of CRT was investigated using chymotrypsin as a conformational probe (Figure 2). Chymotrypsin is a nonmetallo enzyme with sufficiently broad substrate specificity that cleaves preferentially between the carboxyl group of aromatic or leucine residues and the amino group of the adjacent residue (*32*). Digests were carried out at 25 °C in 20 mM Hepes, pH 7.0, 200 mM NaCl, 2 mM EDTA and in 20 mM Hepes, pH 7.0, 200 mM NaCl, 3 mM $MgCl_2$ containing one of the following additives: 1 mM EGTA, 50−1000 μM $CaCl_2$, 400 μM $ZnCl_2$, or 50 μM $CaCl_2$/400 μM $ZnCl_2$. High concentrations of magnesium ions were also added in buffers for proteolytic experiments in order to discriminate between the high- and low-affinity calcium binding sites of CRT. Aliquots were taken at different times, between 0.5 and 12 h, from the reaction mixtures, and samples were analyzed by SDS−PAGE gels (Figure 2).

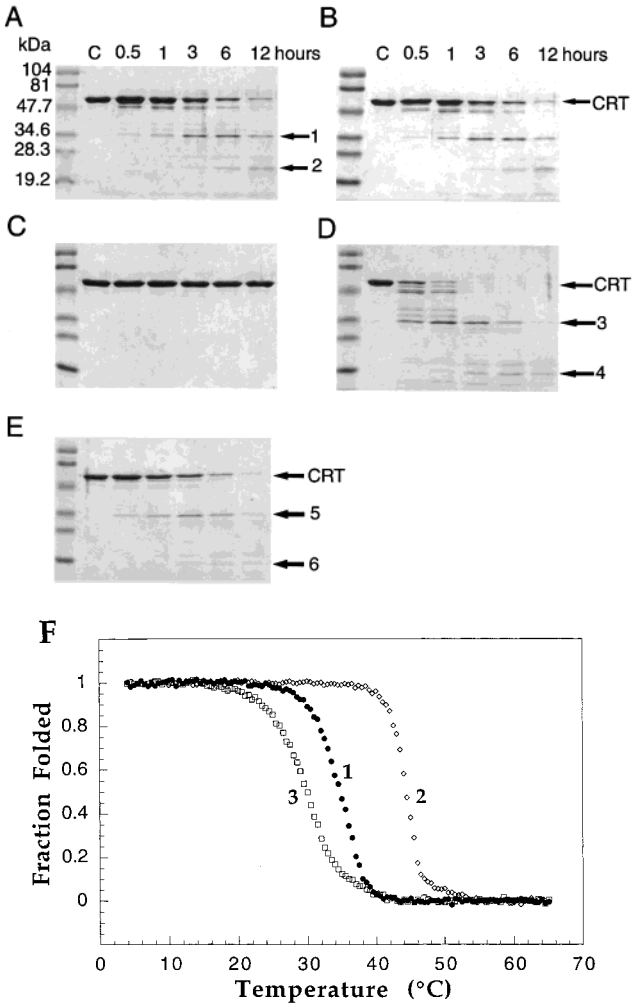

FIGURE 2: SDS−PAGE (12%) analysis of products from chymotrypsin digests carried out at 25 °C using an enzyme:substrate ratio of 1:150 (w/w) in (A) 20 mM Hepes, pH 7.0, 200 mM NaCl, 2 mM EDTA and in 20 mM Hepes, pH 7.0, 200 mM NaCl, 3 mM $MgCl_2$ containing one of the following additives: (B) 1 mM EGTA, (C) 50 μM $CaCl_2$, (D) 400 μM $ZnCl_2$, or (E) 50 μM $CaCl_2$/400 μM $ZnCl_2$. Aliquots were taken at different times from the reaction mixtures as indicated at the top of the figure. Lane C is CRT without added enzymes and loaded at the same concentration as in other lanes. Molecular mass standards are indicated at the left. (F) Thermal denaturation curves (4−65 °C) of CRT obtained by monitoring the change in CD signal at 280 nm. Protein concentrations were 0.4 mg/mL in 20 mM Hepes, pH 7.0, 200 mM NaCl, 3 mM $MgCl_2$ containing one of the following additives: 50 μM $CaCl_2$/400 μM $ZnCl_2$ (curve 1), 50 μM $CaCl_2$ (curve 2), or 400 μM $ZnCl_2$ (curve 3). Curves 2 and 3 are identical to curves 3 and 6, respectively, in Figure 1B. A 1 cm path length cuvette was used to record the denaturation curves.

Results show that incubation of apo CRT with chymotrypsin (Figure 2A) leads to the accumulation of two fragments, migrating at ~35 and ~26 kDa (bands 1 and 2,

Table 1: Identification of Proteolytic Fragments from Chymotrypsin Digests

gel[a]	band[a]	N-terminal cleavage site[b,c]
A	1	^{79}T-V-K-H-E-Q-N
	2	^{166}E-V-K-I-D-N-S
D	3	^{68}S-N-K-G-Q-T-L
		^{79}T-V-K-H-E-Q-N
	4	^{68}S-N-K-G-Q-T-L
		^{79}T-V-K-H-E-Q-N
E	5	^{68}S-N-K-G-Q-T-L
		^{79}T-V-K-H-E-Q-N
	6	^{68}S-N-K-G-Q-T-L
		^{79}T-V-K-H-E-Q-N

[a] Gels and bands shown in Figure 2. [b] Determined by N-terminal amino acid sequencing analysis (7 cycles) after electroblotting samples onto a poly(vinylidene difluoride) membrane (Millipore). [c] Amino acid residues are numbered according to the sequence of full-length recombinant CRT(1−400) without including the additional four N-terminal residues (see Experimental Procedures).

respectively), that remain stable after 12 h incubation. The identities of the fragments corresponding to bands 1 and 2 were established by N-terminal amino acid sequencing, and results revealed that their N-termini correspond to ^{79}T-V-K-H-E-Q-N and ^{166}E-V-K-I-D-N-S (Table 1). On the basis of these results, and of knowledge that CRT and its proteolytic fragments migrate as higher MW species on SDS−PAGE gels (*17, 24, 33*), it can be deduced that fragment corresponding to band 2 results from more extensive cleavage at the N-terminus of CRT, rather than at its C-terminus, in comparison to band 1. Overall, these results suggest that apo CRT is susceptible to proteolytic cleavage by chymotrypsin within its N-domain (Table 1) and to some extent at its C-terminus (C-domain). The pattern of fragmentation obtained for apo CRT is essentially unchanged upon addition of 3 mM $MgCl_2$ (Figure 2B), which is consistent with results obtained from CD studies (Figure 1).

Interestingly, occupancy of the high-affinity calcium site of CRT by the addition of 50 μM $CaCl_2$ (Figure 2C) confers complete resistance to digestion by chymotrypsin even after 12 h incubation as evidenced by the absence of proteolytic fragments in the SDS−PAGE gel. These results suggest that although occupancy of the high-affinity calcium site causes only minor structural rearrangements in CRT (spectrum 3 in Figure 1A), this effect is apparently critical in increasing the conformational rigidity of the protein, at least in the vicinity of the major sites of proteolytic cleavage (bands 1 and 2 in Figure 2A). Identical results as those shown in Figure 2C were obtained when digestion of CRT was carried out in the presence of 1000 μM $CaCl_2$ (data not shown). In marked contrast, the addition of 400 μM $ZnCl_2$ (Figure 2D) results in a significant increase in the susceptibility of CRT to digestion by chymotrypsin as evidenced by the large number of proteolytic fragments produced within the first 0.5 h and by the complete disappearance of the CRT band within the first 3 h. This increased susceptibility of CRT to digestion is consistent with the more pronounced conformational flexibility of the protein upon binding zinc ions as also determined by CD experiments (spectrum 5 in Figure 1A and curve 6 in Figure 1B). Under these conditions, cleavage of CRT by chymotrypsin (Figure 2D) leads to two major proteolytic fragments, with apparent MWs of ~35 and ~18 kDa (bands 3 and 4, respectively), that are mostly absent from the reaction mixture after 12 h incubation. Characterization of fragments corresponding to band 3 by N-terminal amino acid sequencing revealed two distinct N-termini corresponding to ^{68}S-N-K-G-Q-T-L and ^{79}T-V-K-H-E-Q-N (Table 1). The latter fragment (^{79}T-V-K-H-E-Q-N) is most likely identical to that corresponding to band 1 in Figure 2A on the basis of their identical N-termini and migration positions in the SDS−PAGE gel. A characterization of the fragment corresponding to band 4 by N-terminal amino acid sequencing indicated that its N-terminus is identical to the two fragments of band 3, namely, ^{68}S-N-K-G-Q-T-L and ^{79}T-V-K-H-E-Q-N (Table 1). Although these results clearly indicate the more pronounced susceptibility of CRT to cleavage at both its N- and its C-termini upon binding zinc ions, the protein is overall highly destabilized under these conditions.

Collectively, proteolysis results from Figure 2A−D have shown that the backbone conformational flexibility of CRT is intrinsically high and, most notably, can be modulated toward an increase or a decrease in susceptibility to cleavage by chymotrypsin upon binding calcium or zinc ions, respectively.

On the basis of results obtained in Figure 2A−D, it was interesting to determine the proteolytic susceptibility of CRT under conditions in which both calcium and zinc ions were concomitantly added to the solution. SDS−PAGE analysis of products from the digest of CRT carried out in the presence of 50 μM $CaCl_2$/400 μM $ZnCl_2$ (Figure 2E) shows that the kinetics of proteolysis and the overall pattern of fragmentation combine features characteristic of each individual ion as determined in Figure 2C,D. A characterization of the major fragmentation products (bands 5 and 6) by N-terminal amino acid sequencing revealed that their N-termini are identical to the two fragments characterized in Figure 2D (bands 3 and 4, respectively) (Table 1). These studies were further investigated by recording the thermal denaturation curve of CRT in the presence of 50 μM $CaCl_2$/400 μM $ZnCl_2$ (Figure 2F). Results (curve 1) show that under these conditions, both the midpoint temperature (T_m = 34.7 °C) and the steepness of the denaturation transition combine features from the denaturation curves recorded under each separate buffer condition (curves 2 and 3). Taken together, results from Figure 2E,F strongly suggest that neither calcium nor zinc ion completely inhibits the structural effects of the other upon binding to CRT (see also results in Figures 3 and 4 below). This is consistent with the current knowledge that the high-affinity calcium binding site and the low-affinity zinc binding site are located in different regions of CRT (*12, 17*).

Analytical Ultracentrifugation. Our previous characterization of CRT by sedimentation equilibrium and velocity analyses (*24*) clearly established the monodisperse and monomeric nature of the protein as well as its distinctively nonspherical molecular shape. To determine how the binding of calcium and zinc ions by CRT alters its hydrodynamic properties, we have carried out sedimentation velocity analysis (Table 2) in 20 mM Hepes, pH 7.0, 200 mM NaCl, 2 mM EDTA and in 20 mM Hepes, pH 7.0, 200 mM NaCl, 3 mM $MgCl_2$ containing 1 mM EGTA or 50−1000 μM $CaCl_2$. In addition, we have also performed sedimentation velocity (Figure 3) and equilibrium (data not shown) analysis

Table 2: Hydrodymanic Properties of Calreticulin Determined by Sedimentation Analysis[a]

properties	2 mM EDTA(1) (apo CRT)	3 mM $MgCl_2$(2)	50 μM $CaCl_2$(2)	1000 μM $CaCl_2$(2)
sedimentation coefficient ($s^o_{20,w}$)	2.73 ± 0.01 S	2.77 ± 0.01 S	2.80 ± 0.01 S	2.81 ± 0.01 S
Stokes radius (R_S)	45.4 Å	44.7 Å	44.2 Å	44.1 Å
frictional ratio (f/f_0)	1.62	1.60	1.58	1.58
axial ratio (a/b)	11.5	11.1	10.8	10.7
length ($2a$)	286 Å	278 Å	273 Å	271 Å
diameter ($2b$)	24.7 Å	25.0 Å	25.3 Å	25.4 Å

[a] Measurements were done in (1) 20 mM Hepes, pH 7.0, 200 mM NaCl, 2 mM EDTA or in (2) 20 mM Hepes, pH 7.0, 200 mM NaCl, 3 mM $MgCl_2$ containing 1 mM EGTA, 50 μM $CaCl_2$, or 1000 μM $CaCl_2$. The molecular mass (MW) of CRT determined by sedimentation data was 46.0 kDa, which is essentially identical to the MW of 46.8 kDa determined from the amino acid sequence. Hydrodynamic modeling was done using the equation of Perrin for an equivalent, hydrated prolate ellipsoid of revolution (*34*). Values of the partial specific volumes, $V = 0.6950$ cm^3/g (20 °C) and $V = 0.6975$ cm^3/g (25 °C), were calculated from the amino acid composition of human CRT using the consensus partial volumes of the amino acids (*35*) and taking into consideration the expected electrostriction (*36*, *37*) of -0.025 cm^3/g caused by the high net negative charge of about -50/mol of protein (*24*). The degree of hydration, $\delta_1 = 0.502$ g of H_2O/g of protein, was also calculated from the amino acid composition according to Kuntz and Kauzmann (*38*).

of CRT in 20 mM Hepes, pH 7.0, 200 mM NaCl, 3 mM $MgCl_2$ containing 400 μM $ZnCl_2$ or 50 μM $CaCl_2$/400 μM $ZnCl_2$.

Results from sedimentation velocity analysis (Table 2) show that in comparison to apo CRT, the magnesium-saturated form of CRT remains monomeric in solution and is characterized by a slightly larger sedimentation coefficient value, $s^o_{20,w}$, consistent with a somewhat more compact three-dimensional structure. Interestingly, occupancy of the high-affinity calcium site by the addition of 50 μM $CaCl_2$ (Table 2) causes no detectable changes in the overall three-dimensional structure of CRT as indicated by a comparison of its hydrodynamic properties with those of the magnesium-saturated form of the protein. Similarly, binding of calcium ions at the low-affinity calcium site of CRT (Table 2) occurs with no apparent changes in its overall three-dimensional structure in comparison to the magnesium-saturated form of the protein. Since the elongated molecular shape of CRT is unchanged upon binding calcium ions, these results strongly suggest that the calcium-bound form of the protein is likely to retain intrinsic structural plasticity in solution. Noteworthy, our combined results on the metal ion dependency of CRT suggest that although magnesium ions bind to CRT and induce some changes in the secondary and tertiary structures of the protein (Figure 1A,C and Table 2), these effects are not accompanied by a noticeable increase in thermal stability or a change in susceptibility to proteolysis (Figures 1B and 2). This is in marked contrast to the structural effects determined for calcium ions (Figures 1 and 2 and Table 2) and suggests that although magnesium ions bind to the high- and low-affinity calcium sites of CRT, the association is apparently nonspecific.

In marked contrast, sedimentation velocity experiments indicated that the addition of 400 μM $ZnCl_2$ (curve 1 in Figure 3) causes CRT to self-associate reversibly to form dimers as indicated by a concentration dependence of the weight average sedimentation coefficient, $\langle s_{20,w} \rangle$, in the presence of zinc ions. This observation was further investigated by carrying out sedimentation equilibrium analysis at three loading concentrations and two speeds to confirm the monomer−dimer stoichiometry (data not shown). This zinc-induced self-association of CRT determined by sedimentation analysis is consistent with exposure of a hydrophobic surface in the protein and a destabilization of its tertiary structure upon binding zinc ions as suggested by CD and proteolysis experiments (Figures 1A,B, and 2). Interestingly, a concentration-dependent sedimentation velocity analysis carried out in the presence of 50 μM $CaCl_2$/400 μM $ZnCl_2$ (curve 2 in Figure 3) revealed the partial reversible effect that calcium ions exert on the zinc-induced self-association of CRT. This is consistent with results shown in Figure 2E,F (see also results in Figure 4 below) suggesting that upon concomitant binding to CRT, both metal ions can contribute to the overall structural properties of the protein.

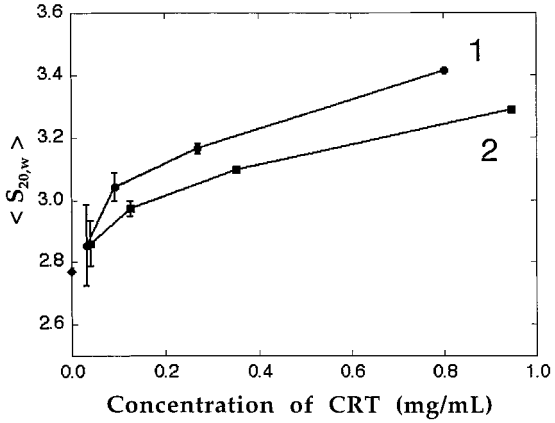

FIGURE 3: Plot of weight average sedimentation coefficient, $\langle s_{20,w} \rangle$, as a function of CRT loading concentrations. Sedimentation velocity experiments were carried out in 20 mM Hepes, pH 7.0, 200 mM NaCl, 3 mM $MgCl_2$ containing 400 μM $ZnCl_2$ (curve 1) or 50 μM $CaCl_2$/400 μM $ZnCl_2$ (curve 2). The isolated point on the *y*-axis (solid diamond) was obtained in 20 mM Hepes, pH 7.0, 200 mM NaCl, 3 mM $MgCl_2$, 1 mM EGTA, a condition under which no self-association of CRT is observed, and therefore represents the value ($s_{20,w} = 2.77$ S) for the monomer (Table 2).

Regulatory Effects of Calcium and Zinc Ions on the Structure of CRT. Results presented above have provided consistent evidence suggesting that the structural properties of CRT can be significantly modulated by interactions with divalent metal ions. These findings were further investigated by recording thermal denaturation curves at 280 nm (Figure 4) using concentrations of concomitantly added calcium and zinc ions in the range 50−1000 and 50−400 μM, respectively, and in the absence of 3 mM $MgCl_2$. Although it is known that the concentration of total calcium ions in the ER is 1 mM, detailed knowledge of the concentration of total zinc ions is surprisingly limited but highly unlikely to be as high as that of calcium ions (*39*−*43*).

Results show that under the different buffer conditions used, the thermal stability of CRT is considerably low and

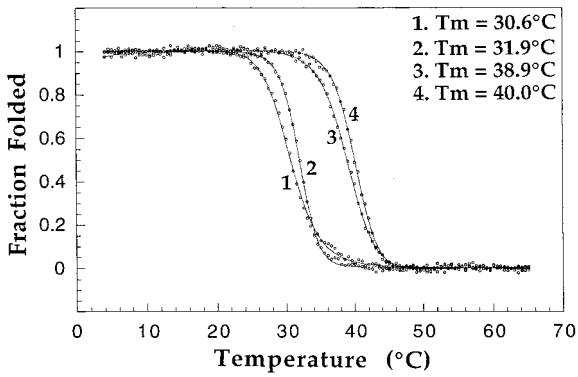

FIGURE 4: Thermal denaturation curves (4−65 °C) of CRT obtained by monitoring the change in CD signal at 280 nm. Protein concentrations were 0.4 mg/mL in 20 mM Hepes, pH 7.0, 200 mM NaCl containing one of the following additives: 50 μM $CaCl_2$/400 μM $ZnCl_2$ (curve 1), 1000 μM $CaCl_2$/400 μM $ZnCl_2$ (curve 2), 50 μM $CaCl_2$/50 μM $ZnCl_2$ (curve 3), 1000 μM $CaCl_2$/50 μM $ZnCl_2$ (curve 4). A 1 cm path length cuvette was used to record the denaturation curves. The theoretical lines through the data points were generated by fitting the denaturation curves to an equation describing a two-state denaturation process (*27, 28*).

varies in the temperature range 30.6−40.0 °C. Results also indicate that the steepness of thermal denaturation transitions is more pronounced at high concentrations of calcium ions (curves 2 and 4) or low concentrations of zinc ions (curve 4), which is consistent with profiles of thermal denaturation curves shown in Figure 1B. These results provide evidence that CRT can effectively respond to a changing cellular environment such as the ER in which homeostatic mechanisms regulate the absorption of calcium and zinc ions (*39*−*41*). However, under all conditions studied, CRT appears to be only marginally stable as evidenced by T_m values that are near physiological temperatures.

DISCUSSION

Using a series of biochemical and biophysical techniques, we have clearly shown that calcium and zinc ions alter the structural properties of CRT in very distinct ways. These results bear functional implications considering that these metal ions are present in the cellular environment of the ER where CRT is active as a chaperone.

More specifically, results from CD measurements, proteolysis studies, and analytical ultracentrifugation analysis (Figures 1 and 2 and Table 2) have shown that occupancy of the high-affinity calcium site in CRT increases the thermal stability and conformational rigidity of the protein, as a consequence of an increase in hydrophobic packing, without changing its overall three-dimensional structure. These results are consistent with the formation of a spatially well-organized site, most likely colocalized with the high-affinity calcium binding site, that is possibly a key feature for expression of the calcium-dependent lectin function of CRT. The formation of a calcium-dependent binding site that is characterized by specific tertiary interactions is also consistent with the very limited number of glycan structures that are known to be recognized by CRT (*20, 44*). Furthermore, the functional importance of this binding site is underscored by considering that the concentration of calcium ions in the lumen of the ER is sufficiently high under all conditions (*45*), that the high-affinity calcium site is constantly occupied by a calcium ion, and, consequently, that the lectin recognition site is intrinsically present in CRT. Finally, this apparent structural dependence of the lectin binding site on occupancy of the calcium ion binding site is a phenomenon known to be active for other lectin binding proteins (*46*−*49*).

Results from CD measurements and analytical ultracentrifugation analysis (Figure 1 and Table 2) have indicated that occupancy of the low-affinity calcium site in the C-domain of CRT further increases the thermal stability and conformational rigidity of the protein, also due to an increase in stabilization of the hydrophobic core, without changing its overall three-dimensional structure. Although the regions of CRT implicated in these structural rearrangements cannot be determined from our studies, knowledge of the CRT structural organization would suggest that these effects can be attributed, at least in part, to changes in the C-domain per se. Results from Figure 1 suggest that calcium ions may serve to spatially organize and stabilize the highly negatively charged C-domain, which was shown to be a more conformationally flexible and destabilized region of the protein in the absence of added calcium ions (Figure 2A,B,D, and refs *24, 31*). The functional implications of these structural rearrangements are not immediately apparent, but they may account for the role that the C-domain has been suggested to play in regulating calcium-dependent interactions between CRT and PDI or ERp57 (*11, 12*). The fluctuating calcium concentrations in the ER would provide a mechanism to control this regulatory process, as also previously suggested (*11, 31*).

In marked contrast to the calcium-induced conformational changes in CRT, results from CD measurements, proteolysis studies, and analytical ultracentrifugation analysis (Figures 1, 2, and 3) have shown that occupancy of the low-affinity zinc site in the N-domain of CRT alters, in a concentration-dependent manner, the internal hydrophobic packing of the protein, resulting in a more expanded tertiary structure with decreased thermal stability. These structural rearrangements increase the hydrophobic character of the protein, causing it to self-associate (Figure 3), and eventually to precipitate at higher concentrations of zinc ions (*10, 12*). Although these conformational changes appear to be more significant than those determined for calcium ions, the protein still retains some highly ordered regions, or domains, under these conditions as evidenced by the magnitude of the ellipticity in the near-UV CD region (spectrum 5 in Figure 1A). As discussed above, although the regions of CRT implicated in these structural rearrangements cannot be localized from our studies, results would suggest that the zinc-dependent structural effects arise, at least in part, from rearrangements in the N-domain per se. The functional implications of the zinc-dependent structural rearrangements determined in our studies are somewhat difficult to address considering that the concentration of total zinc ions in the ER is essentially unknown. However, since our results indicate that concentrations as low as 50 μM $ZnCl_2$ alter the structural properties of CRT (Figures 1B and 4), these effects may be relevant to account for the zinc-dependent interactions between CRT and PDI (*12*). Similarly, the zinc-dependent ability of CRT to suppress the aggregation of unfolded proteins in in vitro assays (*5, 6*) may be accounted for by the exposure of a hydrophobic surface in CRT upon binding zinc ions.

Collectively, these in vitro experiments have highlighted how the extraordinary intrinsic conformational flexibility of CRT can be modulated by the binding of calcium and zinc ions. More specifically, results from Figures 2E,F, 3, and 4 have shown that the concomitant binding of calcium and zinc ions to CRT causes the protein to display structural properties that reflect contributing effects from both metal ions. Overall, the functional significance of these results suggests that CRT may have the intrinsic ability to display two distinct, metal-dependent chaperone functions: a high-affinity calcium-dependent lectin function or a more classical, low-affinity zinc-dependent chaperone function. This would be consistent with recent in vivo studies characterizing the binding properties of the homologue chaperone calnexin (*50*). Just how CRT may utilize two distinct binding sites to facilitate the folding of nascent proteins in the ER is likely to depend on a combination of several contributing factors. As inferred from Figures 2E,F, 3, and 4, and also previously suggested (*11*, *31*), the changing cellular environment of the ER is a mechanism that will effectively modulate the structural properties of CRT. On that basis, the low-affinity calcium and zinc binding sites are likely to be most directly susceptible to metal ion fluctuations. It is also possible that a structural interplay between the lectin and polypeptide binding sites may exist upon association with nascent proteins such that the competence of CRT to express either chaperone function can be altered in order to optimize interactions with the bound protein ligand. This would be consistent, for example, with in vitro studies showing that the binding of isolated oligosaccharides by CRT induces structural re-arrangements in the protein as well as alters its ability to suppress the aggregation of unfolded proteins (*5*).

In summary, these studies have provided new knowledge that allowed us to describe how the structure of CRT responds to interactions with calcium and zinc ions and to discuss how this mechanism could possibly be active in modulating its function as a chaperone in the ER. Our current studies on the biophysical and structural characterization of isolated domains of CRT (V. N. Uversky and M. Bouvier, unpublished results) will provide additional information to further understand the functional implications of the structure of CRT.

ACKNOWLEDGMENT

We thank Dr. Z.-y. Peng and members of his laboratory for permission to use the CD instrument and for discussions, Bill Lane at the Harvard Microchemistry Facility for MALDI mass spectrometry analyses, and Drs. Lars Ellgaard and Vladimir N. Uversky for their comments and suggestions in reading the manuscript.

REFERENCES

1. Nauseef, W. M., McCormick, S. J., and Clark, R. A. (1995) *J. Biol. Chem. 270*, 4741−4747.
2. Wada, I., Imai, S., Kai, M., Sakane, F., and Kanoh, H. (1995) *J. Biol. Chem. 270*, 20298−20304.
3. Peterson, J. R., Ora, A., Van Nguyen, P., and Helenius, A. (1995) *Mol. Biol. Cell 6*, 1173−1184.
4. Hebert, D. N., Foellmer, B., and Helenius, A. (1996) *EMBO J. 15*, 2961−2968.
5. Saito, Y., Ihara, Y., Leach, M. R., Cohen-Doyle, M. F., and Williams, D. B. (1999) *EMBO J. 18*, 6718−6729.
6. Svaerke, C., and Houen, G. (1998) *Acta Chem. Scand. 52*, 942−949.
7. Smith, M. J., and Koch, G. L. E. (1989) *EMBO J. 8*, 3581−3586.
8. Fliegel, L., Burns, K., MacLennan, D. H., Reithmeier, R. A. F., and Michalak, M. (1989) *J. Biol. Chem. 264*, 21522−21528.
9. Michalak, M. (1996) in *Calreticulin*, R. G. Landes Co., Austin, TX.
10. Khanna, N. C., Tokuda, M., and Waisman, D. M. (1986) *J. Biol. Chem. 261*, 8883−8887.
11. Corbett, E. F., Oikawa, K., Francois, P., Tessier, D. C., Kay, C., Bergeron, J. J. M., Thomas, D. Y., Krause, K.-H., and Michalak, M. (1999) *J. Biol. Chem. 274*, 6203−6211.
12. Baksh, S., Burns, K., Andrin, C., and Michalak, M. (1995) *J. Biol. Chem. 270*, 31338−31344.
13. Ellgaard, L., Riek, R., Braun, D., Hermann, T., Helenius, A., and Wuthrich, K. (2001) *FEBS Lett. 488*, 69−73.
14. Ellgaard, L., Riek, R., Hermann, T., Guntert, P., Braun, D., Helenius, A., and Wuthrich, K. (2001) *Proc. Natl. Acad. Sci. U.S.A. 98*, 3133−3138.
15. Ostwald, T. J., MacLennan, D. H., and Dorrington, K. J. (1974) *J. Biol. Chem. 249*, 5867−5871.
16. Ostwald, T. J., and MacLennan, D. H. (1974) *J. Biol. Chem. 249*, 974−979.
17. Baksh, S., and Michalak, M. (1991) *J. Biol. Chem. 266*, 21458−21465.
18. Khanna, N. C., Tokuda, M., and Waisman, D. M. (1987) *Biochem. J. 242*, 245−251.
19. Van Nguyen, P., Peter, F., and Söling, H.-D. (1989) *J. Biol. Chem. 264*, 17494−17501.
20. Vassilakos, A., Michalak, M., Lehrman, M. A., and Williams, D. B. (1998) *Biochemistry 37*, 3480−3490.
21. Peterson, J. R., and Helenius, A. (1999) *J. Cell Sci. 112*, 2775−2784.
22. McCauliffe, D. P., Lux, F. A., Lieu, T.-S., Sanz, I., Hanke, J., Newkirk, M. M., Bachinski, L. L., Itoh, Y., Siciliano, M. J., Reichlin, M., Sontheimer, R. D., and Capra, J. D. (1990) *J. Clin. Invest. 85*, 1379−1391.
23. Treves, S., DeMattei, M., Lanfredi, M., Villa, A., Green, N. M., MacLennan, D. H., Meldolesi, J., and Pozzan, T. (1990) *Biochem. J. 271*, 473−480.
24. Bouvier, M., and Stafford, W. (2000) *Biochemistry 39*, 14950−14959.
25. Waisman, D. M., Salimath, B. P., and Anderson, M. J. (1985) *J. Biol. Chem. 260*, 1652−1660.
26. Edelhoch, H. (1967) *Biochemistry 6*, 1948−1954.
27. Bouvier, M., and Wiley, D. C. (1994) *Science 265*, 398−402.
28. Bouvier, M., and Wiley, D. C. (1998) *Nat. Struct. Biol. 5*, 377−384.
29. Stafford, W. F. (1994) *Methods Enzymol. 240*, Part B, 478−501.
30. Brenner, S. L., Zlotnick, A., and Stafford, W. F. (1990) *J. Mol. Biol. 216*, 949−964.
31. Corbett, E. F., Michalak, K. M., Oikawa, K., Johnson, S., Campbell, I. D., Eggleton, P., Kay, C., and Michalak, M. (2000) *J. Biol. Chem. 275*, 27177−27185.
32. Smith, D. G. (1967) *Methods Enzymol. 11*, 214−231.
33. Rokeach, L. A., Haselby, J. A., and Hoch, S. O. (1991) *Protein Eng. 4*, 981−987.
34. Stafford, W. F., and Schuster, T. M. (1995) in Hydrodynamic Transport Methods. in *Introduction to Physical Methods for Protein and Nulceic Acid Research* (Glaser, J. A., and Deutscher, M. P., Eds.) Academic Press Inc., Orlando, FL.
35. Perkins, S. J. (1986) *Eur. J. Biochem. 157*, 169−180.
36. Cohn, E. J., and Edsall, J. T. (1943) in *Proteins, Amino Acids and Peptides*, pp 370−381, Reinhold Publishing Corp., New York.
37. Laue, T. M. (1992) in *Analytical Ultracentrifugation in Biochemistry and Polymer Science* (Harding, S. E., Rowe, A. J., and Horton, J. C., Eds.) pp 63−89, Royal Society of Chemistry, Cambridge, U.K.
38. Kuntz, I. D., Jr., and Kauzmann, W. (1974) *Adv. Protein Chem. 28*, 239−345.

39. Carafoli, E. (1987) *Annu. Rev. Biochem. 56*, 395−443.
40. Berridge, M. J. (1993) *Nature 361*, 315−325.
41. Pozzan, T., Rizzuto, R., Volpe, P., and Meldolesi, J. (1994) *Physiol. Rev. 74*, 595−636.
42. Vallee, B. L., and Falchuk, K. H. (1993) *Physiol. Rev. 73*, 79−118.
43. Smeyers-Verbeke, J., May, C., Drochmans, P., and Massart, D. L. (1977) *Anal. Biochem. 83*, 746−753.
44. Spiro, R. G., Zhu, Q., Bhoyroo, V., and Soling, H. D. (1996) *J. Biol. Chem. 271*, 11588−11594.
45. Meldolesi, J., and Pozzan, T. (1998) *Trends Biochem. Sci. 23*, 10−14.
46. Kalb, A. J., and Levitzki, A. (1968) *Biochem. J. 109*, 669−672.
47. Ng, K. K.-S., Park-Snyder, S., and Weis, W. I. (1998) *Biochemistry 37*, 17965−17976.
48. Anostario, M., Jr., and Huang, K.-S. (1995) *J. Biol. Chem. 270*, 8138−8144.
49. Mullin, N. P., Hall, K. T., and Taylor, M. E. (1994) *J. Biol. Chem. 269*, 28405−28413.
50. Danilczyk, U. G., and Williams, D. B. (2001) *J. Biol. Chem. 276*, 25532−25540.

BI010948L